ARTICLE

Preparation of TiO_2/Bi_2O_3 Microfibers and Their Photocatalytic Activity

Zhan-ying Ma*, Ling-juan Deng, Xiao-bo Li, Guang Fan*

College of Chemistry and Chemical Engineering, Xianyang Normal University, Xianyang 712000, China

(Dated: Received on March 12, 2014; Accepted on May 8, 2014)

A series of TiO_2/Bi_2O_3 heterojunction microfibers have been fabricated using cotton fibers as bio-templates, and characterized by XRD, SEM and UV-Vis techniques. Results reveal that Bi_2O_3 in the TiO_2/Bi_2O_3 sample is assigned to monoclinic and tetragonal mix-crystal phase. Fibers lengths can reach several micrometers and diameters range from 0.5 μm to 3 μm. Compared with pure TiO_2 and Bi_2O_3, TiO_2/Bi_2O_3 samples display better absorption in visible light region. Photocatalytic activity was evaluated by degradation of MB under visible light irradiation. TiO_2/Bi_2O_3 microfibers exhibite much higher activity than pure TiO_2 and Bi_2O_3, and 22.84%TiO_2/Bi_2O_3 can achieve the decomposition of about 95%MB, which is attributed to synergistic effects of the strong visible-light absorption of TiO_2/Bi_2O_3 microfibers and the heterojunction formed between TiO_2 and Bi_2O_3.

Key words: TiO_2/Bi_2O_3 microfiber, Visible light, Heterojunction, Photocatalysis

I. INTRODUCTION

During the past decades, semiconductor photocatalytic process has been proven a promising method in the destruction of organic pollutants in wastewater due to its strong oxidation power, moderate operation temperature, and relative "green" final products. Bismuth oxide (Bi_2O_3) is an attractive semiconductor material with a direct band-gap of 2.8 eV [1], which can be excited by visible light, and is widely used for pollutant decomposing under visible light irradiation [2, 3]. The band value provides the potential for the generation of reactive radicals, $O_2^{\cdot -}$ and $OH^{\cdot}$, in photocatalytic reactions. However, the photocatalytic activity of Bi_2O_3 is low due to the photocorrosion and recombination of photogenerated electron-hole pairs. So its efficiency under visible light is required to be improved for the cost-effective removal of specific organic contaminants. To improve of charge separation, increase charge carrier lifetime, and thus enhance photocatalytic activity due to high efficiency of the interfacial charge transfer from catalyst to adsorbed substrates, coupled semiconductor photocatalysts have been used [4]. To date, the most commonly used TiO_2 have been extensively chosen as potential candidate for forming diverse heterojunctions in photocatalysts because of its non-toxic and stability nature [5]. Recently, efforts have been made to look for the possibility of Bi_2O_3-TiO_2 combination in a photocatalyst, and its efficiency to degrade methyl orange (MO) has been reported [6].

It is well known that the morphology of materials has an important effect on its catalytic property [7, 8]. Therefore, great efforts have been made to combine TiO_2 and Bi_2O_3 with different morphologies [8, 9]. Microfibers, an important subclass of microstructure materials, have several advantages such as increasing the interactive surface area between photocatalyst material and target pollutant, providing more active sites, and facilitating degradation product molecule diffusion, which could probably enhance their photocatalytic activity. Photocatalysts with nano- or micro-fiber structure have been fabricated [10, 11].

Template procedures are an ideal way to control material structure, including the outer morphology, size, the inner pore size, and distribution [12]. In recent years, natural living things (such as cotton [10, 13], silk [14], wood [15], paper [16], *etc.*), are commonly used as template, which are easily removed with heating procedures. Cotton template has been proven useful for the formation of nanofibers [10] or microtubes [13].

In this work, TiO_2/Bi_2O_3 heterojunction photocatalysts with microfiber morphology were produced with cotton as the template to enhance their photocatalytic activity. The photocatalytic property of TiO_2/Bi_2O_3 heterojunctions was tested by the degradation of methylene blue (MB) under visible light irradiation, and compared with pure Bi_2O_3 and TiO_2. 22.84%TiO_2/Bi_2O_3 heterojunction shows superior visible-light absorption and higher photocatalytic activity in the degradation of MB. Moreover, the possible reasons for the enhanced photocatalytic activity of TiO_2/Bi_2O_3 heterojunction were also discussed.

II. EXPERIMENTS

All chemicals were analytical reagent grade and used as received without further purification. In a typical

*Authors to whom correspondence should be addressed. E-mail: fanguang2004@163.com, mazhanying@163.com, Tel.: +86-29-33720371

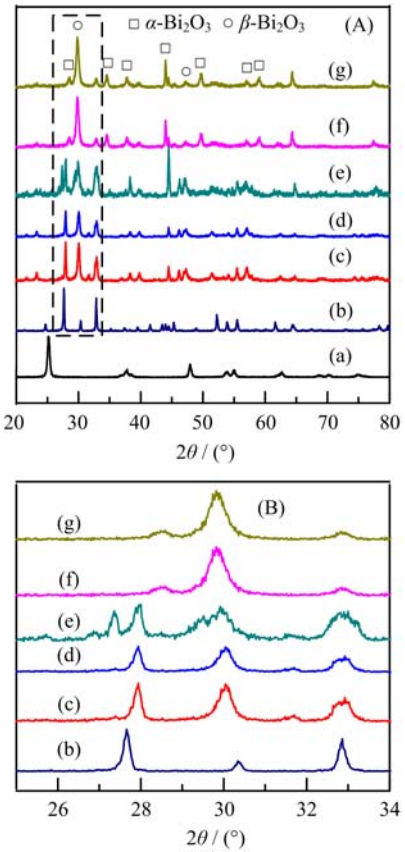

FIG. 1 XRD patterns of pure TiO_2, pure Bi_2O_3 and TiO_2/Bi_2O_3 composites. (a) Pure TiO_2, (b) pure Bi_2O_3, (c) 5.71%TiO_2/Bi_2O_3, (d) 11.42%%TiO_2/Bi_2O_3, (e) 17.12%TiO_2/Bi_2O_3, (f) 22.84%TiO_2/Bi_2O_3, and (g) 28.53%TiO_2/Bi_2O_3.

procedure, 0.485 g of $Bi(NO_3)_3{\cdot}5H_2O$ and 0.384 g of citric acid were dissolved in nitric acid aqueous solution, the pH was adjusted to 7.0 by dropwisely titration of ammonia solution under stirring, and transparent solution A was formed. Different dosage of n-tetrabutyltitanate ($C_{16}H_{36}O_4Ti$) was dissolved in ethanol at room temperature, thus pale-yellow solution B was formed. The dried and loose cotton fibers were immersed into the mixture of solution A and B. After immersing for 24 h, the cotton fibers were taken out, dried at 50 °C for 12 h, which were then placed in an alundum crucible and calcined in air at 500 °C for 1 h. Finally, pale-yellow TiO_2/Bi_2O_3 heterojunction were obtained. These as-synthesized materials were denoted as $x$$TiO_2/Bi_2O_3$, x indicates the molar ratio.

The phase identification of the as-prepared powders were obtained on a Riggaku D/max-3C X-ray powder X-ray diffractometry using Cu Kα radiation (λ=1.5405 Å, 40 kV, 40 mA). Scanning electron microscopy (SEM) images were observed by Hitachi S-4800 scanning electron microscopy. UV-visible diffuse reflectance spectra (UV-DRS) of the samples were recorded on Lambd 950 spectrophotometer using $BaSO_4$ as reference.

The photocatalytic activity of TiO_2/Bi_2O_3 heterojunctions was evaluated by measuring the degradation of the MB under visible-light irradiation. In a typical process, 100 mg TiO_2/Bi_2O_3 samples were added to 100 mL of 10 mg/L MB solution and then bubbled in the dark for 20 min, to reach adsorption equilibrium and uniform dispersity. The solution was then exposed to visible light irradiation from a 300 W Xe lamp at room temperature. At given time intervals (20 min), 5 mL of the suspension was withdrawn and centrifuged to remove the photocatalyst powders for analysis. The concentration of MB was monitored using UV-Vis spectrophotometry by measuring the absorbance at 664 nm.

III. RESULTS AND DISCUSSION

A. Crystal structure

XRD is used to determine the phase structure of the samples. Figure 1 shows XRD patterns of pure TiO_2, pure Bi_2O_3, and TiO_2/Bi_2O_3 heterojunctions. All the peaks of the pure TiO_2 sample are assigned to the anatase TiO_2 (PDF No.21-1272) and those of pure Bi_2O_3 are indexed to two distinct crystal phases monoclinic α-Bi_2O_3 (PDF No.76-1730) and tetragonal β-Bi_2O_3 (PDF No.76-147). In the case of TiO_2/Bi_2O_3 composites, all the intensive and sharp reflection peaks can match well with pure Bi_2O_3 (mixed crystal phase), and the characteristic peaks observed for α-Bi_2O_3 are assigned to diffraction from the (002), (041), (104), and (212) planes [17]. The characteristic peaks of β-Bi_2O_3 correspond to the diffraction from the (211), (220), (400), and (402) planes [18].

With increasing the contents of TiO_2 in the composites, diffraction peaks of TiO_2/Bi_2O_3 composites shift slightly (Fig.1), compared with those of pure Bi_2O_3, which may be attributed to the formation of p-n heterojunction which leads to the lattice distortion. No TiO_2 diffraction peaks are detected in the TiO_2/Bi_2O_3 pattern, which may be ascribed to low TiO_2 content [19]. In addition, as shown in Fig.1, no other diffraction peaks of Bi related impurities are noted, which confirm the complete decomposition of bismuth nitrate to bismuth oxide.

B. SEM observation

Morphologies of as-prepared samples are investigated with SEM, and their typical images are displayed in Fig.2. It can be observed that these TiO_2/Bi_2O_3 composites were consisted of a large quantity of microfiber structures. Their lengths can reach several micrometers and diameters range from 0.5 μm to 3 μm. The surfaces of these microfibers are coarse and have many microstructures on them. Furthermore, the SEM images obtained with different dosage of TiO_2 show no

DOI:10.1063/1674-0068/27/04/439-444

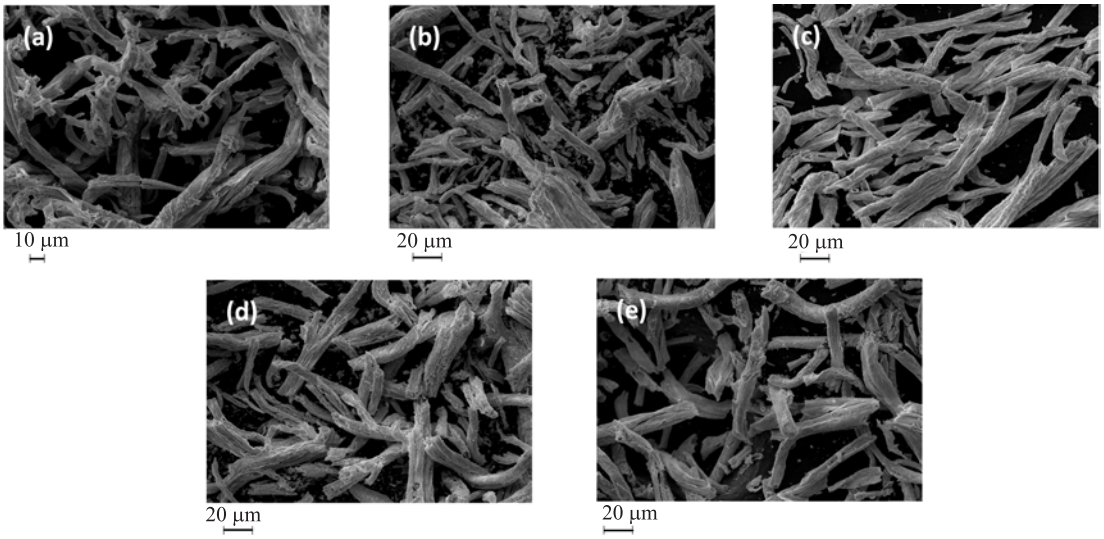

FIG. 2 SEM images of TiO_2/Bi_2O_3 microfibers obtained with different dosage of TiO_2. (a) 5.71%TiO_2/Bi_2O_3, (b) 11.42%TiO_2/Bi_2O_3, (c) 17.12%TiO_2/Bi_2O_3, (d) 22.84%TiO_2/Bi_2O_3, and (e) 28.53%TiO_2/Bi_2O_3.

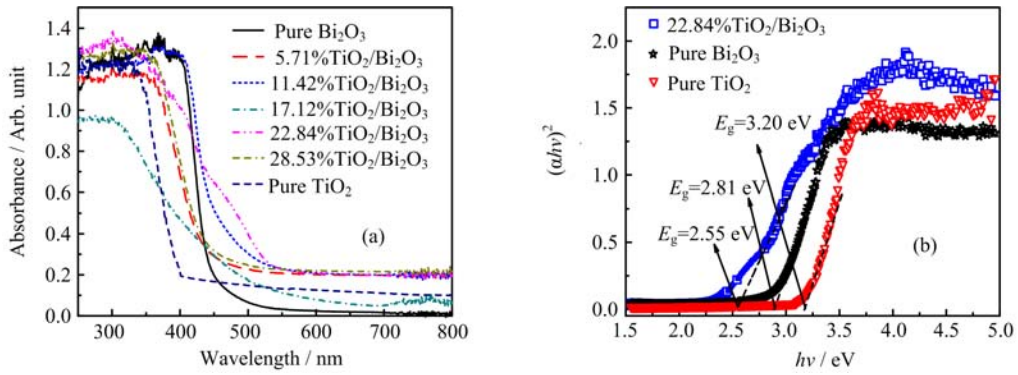

FIG. 3 (a) UV-Vis diffuse reflectance spectra and (b) the band gap energies (E_g) of the pure TiO_2, Bi_2O_3, and TiO_2/Bi_2O_3 composites.

notable differences. All these TiO_2/Bi_2O_3 microfibers present as straight or twisted shapes, which are well consistent with the straight or twisted shapes of cotton template, indicating the formation of biomorphic TiO_2/Bi_2O_3 microfibers via cotton template.

C. UV-Vis DRS analysis

Figure 3(a) demonstrates the UV-Vis DRS spectra of the pure Bi_2O_3, pure TiO_2 and TiO_2/Bi_2O_3 heterostructures. It is shown that, pure TiO_2 displays no absorption of visible-light. While Bi_2O_3 and a series of TiO_2/Bi_2O_3 heterostructures display prominent photoabsorption ability in the visible region, implying that they have the potential to be efficient visible-light-driven photocatalysts. In addition, among them, 22.84%TiO_2/Bi_2O_3 heterostructure present a better visible light absorption performance.

Based on the DRS data, as shown in Fig.3(b), the band gaps of pure TiO_2, pure Bi_2O_3 and 22.84%TiO_2/Bi_2O_3 composites are estimated to be 3.20, 2.89 and 2.55 eV based on the following formula [20]:

$$\alpha h\nu = A(h\nu - E_g)^{n/2} \quad (1)$$

The change in the band gap values is ascribed to the introduction of TiO_2 into Bi_2O_3. The formation of heterojunction between Bi_2O_3 and TiO_2 narrows the band gap and extends the optical absorption range. Thus the results further indicate that TiO_2/Bi_2O_3 composite photocatalyst has a wider photoabsorption range and more suitable band gap for photocatalytic applications.

D. Photocatalytic properties

1. Photocatalytic activities

The photocatalytic activities of as-prepared photocatalysts were evaluated for degradation of MB un-

DOI:10.1063/1674-0068/27/04/439-444

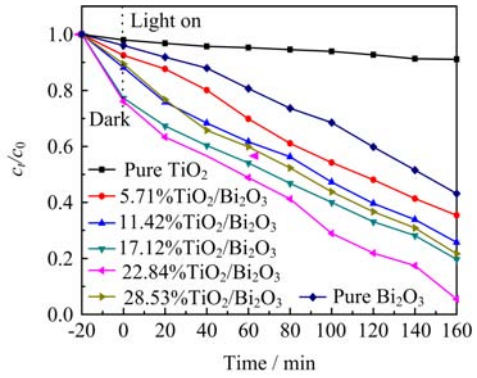

FIG. 4 Visible-light photocatalytic activities of pure TiO_2, pure Bi_2O_3 and TiO_2/Bi_2O_3 composites for the degradation of MB.

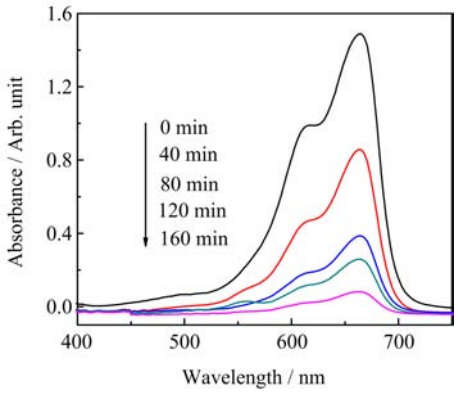

FIG. 5 UV-Vis absorption of the MB aqueous solutions under visible light irradiation in the presence of 22.84%TiO_2/Bi_2O_3 for different time.

der visible light. Figure 4 exhibited the plots of c_t/c_0 versus irradiation time for different samples, where c_0 and c_t is the MB concentration before and after irradiation. As can be seen from Fig.4, TiO_2 exhibits no visible-light-driven photocatalytic activity, but all the TiO_2/Bi_2O_3 heterojunctions and pure Bi_2O_3 exhibit considerably high photocatalytic activities in the decomposition of MB under visible light irradiation. What's more, the photocatalytic activities of TiO_2/Bi_2O_3 heterojunctions are all higher than that of pure Bi_2O_3. 22.84%TiO_2/Bi_2O_3 exhibits the highest photocatalytic activity, which can achieve the decomposition of about 95% MB upon visible light irradiation for 160 min.

There are two possibile machanisms, that is photocatalytic decomposition of MB, and production of the doubly reduced form of MB, *leuco*-MB [21]. With the addition of $AgNO_3$ into the system, the solution was not recovered to blue, indicating that the MB was not reduced to *leuco*-MB, which can be reversibly oxidized to MB by $AgNO_3$ [22]. Figure 5 shows the evolution of MB absorption spectra, from which it could be seen that the absorption peak of MB at 664 nm drops rapidly in the presence of 22.84%TiO_2/Bi_2O_3. This indicates that the MB dye is photocatalytically decomposed by 22.84%TiO_2/Bi_2O_3. The color of the dispersion almost disappears after 160 min of irradiation, indicating that the chromophoric structure of the dye was destroyed.

2. Photocatalytic mechanism

In order to investigate the mechanism of the enhanced photocatalytic activity of heterojunction, the relative band position of the two semiconductors should be confirmed, because the band-edge potential positions play an important part in determining the flowchart of photoinduced charge carriers in the heterojunction structure [23, 24]. The band edge positions of conduction band (CB) and valence band (VB) of the semiconductor at the point of zero charge can be calculated by the empirical equation [25, 26]:

$$E^0_{\rm CB} = \chi - E_{\rm C} - \frac{1}{2}E_{\rm g} \qquad (2)$$

where χ is the absolute electro-negativity of the semiconductor (χ is 5.90 and 6.09 eV for TiO_2 and Bi_2O_3, respectively [9]). $E_{\rm C}$ is the energy of free electrons on the hydrogen scale (4.5 eV), and $E_{\rm g}$ is the band-gap of the semiconductor. Therefore, according to the Eq.(2), the calculated CB and VB of TiO_2 are -0.2 and 3.00 eV, and those of Bi_2O_3 are 0.18 and 2.99 eV, respectively.

The improved performance observed over the TiO_2/Bi_2O_3 composite compared to pure TiO_2 and Bi_2O_3 can be ascribed to formation of the p-n junction. When p-type Bi_2O_3 and n-type TiO_2 are contacted, the Fermi level of p-type Bi_2O_3 moves up, while in the meantime, that of n-type TiO_2 moves down until the equilibrium state is formed. Consistent with the moving of the Fermi level, the whole energy band of p-type Bi_2O_3 is raised up, while that of n-type TiO_2 is descended. An inner electric field from n-type TiO_2 to p-type Bi_2O_3 is thus established. The activity enhancement of Bi_2O_3 was ascertained owing to this high efficient separation mode for TiO_2/Bi_2O_3 heterojunction [27]. According to the schematic diagram in Fig.6, under visible light irradiation, only Bi_2O_3 could be activated and induce the generation of electron-hole pairs. The produced electrons on the CB of Bi_2O_3 are transferred to that of TiO_2, whereas h^+ still remains in the VB of Bi_2O_3. Thus, the separation of e^- and h^+ in Bi_2O_3 can be promoted, and accordingly their recombination is reduced. The more efficient separation of e^- and h^+ can increase their lifetimes and enhance the efficiency of their transfer to the adsorbed substrates. Similar mechanism was presented for $BiOI/TiO_2$ [28] and Bi_2WO_6/TiO_2 [29]. Hence, it is reasonable that Bi_2O_3/TiO_2 composites can exhibit higher photocatalytic efficiencies than pure TiO_2 under visible light irradiation.

With regard to the difference in the photocatalytic

DOI:10.1063/1674-0068/27/04/439-444

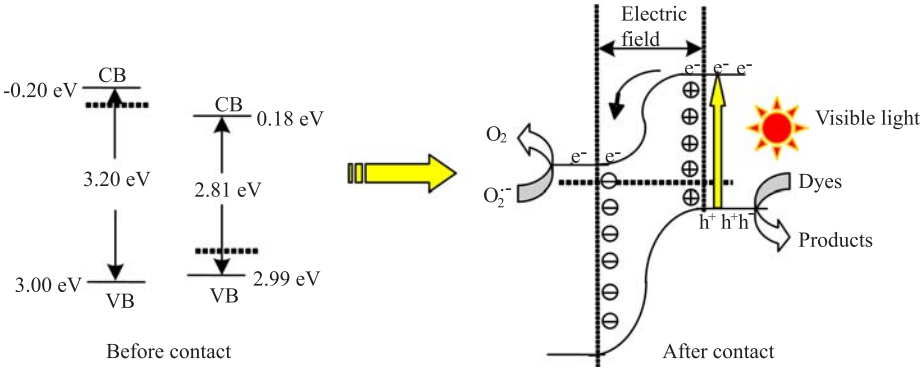

FIG. 6 Schematic diagram of separation of electron-hole pairs over TiO_2/Bi_2O_3 p-n junction under visible light irradiation.

activities of TiO_2/Bi_2O_3 heterojunctions, it should be attributed to the combined action of many factors, such as composition, size, specific area, and adsorption capacity for MB, *etc.* Since all the other influencing factors (*e.g.*, size, specific surface area and adsorption capacity, *etc.*) are also dependent on the composition. It is believed that the composition of Bi_2O_3/TiO_2 heterojunctions should play a dominant role in their photocatalytic activities. Bi_2O_3 possesses relatively high visible-light-driven photocatalytic activity in the degradation of MB, whereas TiO_2 has no photocataltic activity under visible light irradiation. When TiO_2 content is too low (*e.g.*, 5.71%TiO_2/Bi_2O_3, 11.42%TiO_2/Bi_2O_3), Bi_2O_3 cannot contact "enough amount" of TiO_2 or the surface of Bi_2O_3 is insufficiently covered with TiO_2, which restricts the efficient interfacial electron transfer from Bi_2O_3 to TiO_2. On the other hand, too much TiO_2 possibly blocks the incident light irradiation on Bi_2O_3. Therefore, when TiO_2/Bi_2O_3 heterojunctions have a too high content of TiO_2 (*e.g.*, 28.53%TiO_2/Bi_2O_3), they cannot accomplish the highest photocatalytic efficiency [30]. Therefore, there must be an optimum composition for TiO_2/Bi_2O_3 heterojunctions to achieve the highest photocatalytic efficiency. In this work, 22.84%TiO_2/Bi_2O_3 with a suitable content of TiO_2 exhibits the highest photocatalytic efficiency among a series of TiO_2/Bi_2O_3 heterojunctions.

IV. CONCLUSION

A heterojunction photocatalyst with microfiber structure is prepared using cotton fibers as biotemplates. Introduction of TiO_2 to Bi_2O_3 don't change the crystalline structure of Bi_2O_3, but extend the photoabsorption region apparently. Photocatalytic experiments show that TiO_2/Bi_2O_3 heterojunction exhibites enhanced photocatalytic activity compared with pure Bi_2O_3, and 22.84%TiO_2/Bi_2O_3 exhibited the highest photocatalytic activity towards the degradation of MB, and 95%MB can be degraded within 160 min. Based on the UV-Vis DRS data, a possible photocatalytic mechanism is proposed. The enhanced photocatalytic activity of 22.84%TiO_2/Bi_2O_3 is mainly ascribed to the effective separation of photoinduced electron-hole pairs at the interface of heterojunction. Besides, the wider photoabsorption range and better crystallinity also favor its excellent photocatalytic performance. This work provides a new insight for developing novel composite catalyst, as well as offering high efficient visible-light-driven photocatalysts for water purification and environmental remediation.

V. ACKNOWLEDGEMENTS

This work was supported by the Scientific Research Program Funded by Shaanxi Provincial Education Department (No.2013JK0690), and the Shaanxi Province Natural Science Foundation (No.2013JM2013), the National Natural Science Foundation of China (No.21203160), and the Special Research Fund of Xianyang Normal University (No.11XSYK204).

[1] A. Hameed, V. Gombac, T. Montini, L. Felisri, and P. Fornasiero, Chem. Phys. Lett. **483**, 254 (2009).
[2] L. S. Zhang, W. Z. Wang, J. Yang, Z. G. Chen, W. Q Zhang, L. Zhou, and S. W. Liu, Appl. Catal. A **308**, 105 (2006).
[3] Z. Y. Ma, B. H. Yao, Y. Q. He, H. N. Bai, and Y. H. Gao, J. Funct. Mater. **44**, 507 (2013).
[4] Y. Bessekhouad, D. Robert, and J. V. Weber, Catal. Today **101**, 315 (2005).
[5] M. Qin, W. Zhao, J. L. Chu, J. K. Qu, L. N. Wang, S. H. Li, H. Zhang, and H. X. Zhao, Mater. Res. Bull. **48**, 1076 (2013).
[6] S. Shamaila, A. K. L. Sajjad, F. Chen, and J. L. Zhang, Appl. Catal. B **94**, 272 (2010).
[7] B. Naik, S. Martha, and K. M. Parida, Int. J. Hydrogen Energy **36**, 2794 (2011).
[8] J. Zhu, S. Wang, J. Wang, D. Zhang, and H. Li, Appl. Catal. B **102**, 120 (2011).

DOI:10.1063/1674-0068/27/04/439-444

[9] G. P. Dai, S. Q. Liu, R. Peng, and T. X. Luo, Acta Phys. Chim. Sin. **28**, 2169 (2012).
[10] B. T. Su, K. Wang, N. Dong, H. M. Mu, Z. Q. Lei, Y. C. Tong, and J. Bai, J. Mater. Process. Tech. **209**, 4088 (2009).
[11] Y. J. Li, Z. H. Zhang, T. P. Cao, C. L. Shao, and L. M. Wei, Chin. J. Inorg. Chem. **27**, 1348 (2011).
[12] S. Polarz and M. Antonietti, Chem. Commun. **22**, 2593 (2002).
[13] L. J. Xie, W. Chu, Y. Y. Huang, and D. G. Tong, Mater. Lett. **65**, 153 (2011).
[14] Q. Xu, J. B. Li, Q. Peng, L. L. Wu, and S. P. Li, Mater. Sci. Eng. B **127**, 212 (2006).
[15] Z. T. Liu, T. X. Fan, D. Zhang, X. L. Gong, and J. Q. Xu, Sensors Actuators B **136**, 499 (2009).
[16] J. Li, F. L. Kwong, and D. H. L. Ng, J. Am. Ceramic Soc. **91**, 1350 (2008).
[17] P. P. Xiao, L. L. Zhu, Y. C. Zhu, and Y. T. Qian, J. Solid State Chem. **184**, 1459 (2011).
[18] Y. F. Qiu, M. L.Yang, H. B. Fan, Y. Z. Zuo, Y. Y. Shao, Y. J. Xu, X. X. Yang, and S. H. Yang, Mater. Lett. **65**, 780 (2011).
[19] Q. Mi, D. Q. Chen, J. C. Hu, Z. X. Huang, and J. L. Li, Chin. J. Catal. **34**, 2138 (2013).
[20] A. Mills, R. H. Davies, and D. Worsley, Chem. Soc. Rev. **22**, 417 (1993).
[21] A. Mills and J. S. Wang, J. Photochem. Photobiol. A **127**, 123 (1999).
[22] B. Muktha, T. Aarthi, G. Madras, and T. N. G. Row, J. Phys. Chem. B **110**, 10280 (2006).
[23] M. S. Gui, W. D. Zhang, Y. Q. Chang, and Y. X. Yu, Chem. Eng. J. **197**, 283 (2012).
[24] X. J. Su, X. X. Zou, G. D. Li, X. Wei, C. Yan, Y. N. Wang, J. Zhao, L. J. Zhou, and J. S. Chen, J. Phys. Chem. C **115**, 8064 (2011).
[25] M. A. Butler and D. S. Ginley, J. Electrochem. Soc. **125**, 228 (1978).
[26] T. B. Li, G. Chen, C. Zhou, Z. Y. Shen, R. C. Jin, and J. X. Sun, Dalton Transactions **40**, 6751 (2011).
[27] J. Jiang, X. Zhang, P. B. Sun, and L. Z. Zhang, J. Phys. Chem. C **115**, 20555 (2011).
[28] G. P. Dai, J. G. Yu, and G. Liu, J. Phys. Chem. C **115**, 7339 (2011).
[29] Q. C. Xu, D. V. Wellia, Y. H. Ng, R. Amal, and T. T. Y. Tan, J. Phys. Chem. C **115**, 7419 (2011).
[30] Y. C. Zhang, L. Yao, G. Zhang, D. D. Dionysiou, J. Li, and X. H. Du, Appl. Catal. B **144**, 730 (2014).

DOI:10.1063/1674-0068/27/04/439-444